

# Optimizing the Pulsed Current GTAW Process Parameters to Attain Maximum Tensile Strength Using RSM

<sup>1</sup>V. Subravel\*, <sup>1</sup>G. Padmanaban and <sup>2</sup>V. Balasubramanian

<sup>1</sup>Assistant Professor, Centre for Materials Joining & Research (CEMAJOR), Department of Manufacturing Engineering, Annamalai University, Annamalainagar- 608002, Tamil Nadu, India

<sup>2</sup>Professor, Centre for Materials Joining & Research (CEMAJOR), Department of Manufacturing Engineering, Annamalai University, Annamalainagar- 608002, Tamil Nadu, India

\*Corresponding Author Email: subra.vetri@gmail.com

## ABSTRACT

In this investigation, an attempt has been made to predict the tensile strength of pulsed current gas tungsten arc welded (PCGTAW) AZ31B magnesium alloy joints using RSM incorporating process parameters such as peak to base current ratio, welding speed, pulse frequency and pulse on time as variables. The experiments were conducted based on a four-factor, five-level, central composite design matrix. The developed empirical relationship can be effectively used to predict the tensile strength of PCGTAW joints of AZ31B magnesium alloy at 95% confidence level. The results indicated that welding speed and pulse frequency has the greatest influence on tensile strength, followed by current ratio, pulse on time. Response surface methodology (RSM) was used to optimize PCGTAW parameters to attain a maximum tensile strength of 214 MPa (78 % of base metal strength) in the AZ31B Magnesium alloy joints.

**Key words:** AZ31B magnesium alloy; pulsed current gas tungsten arc welding; response surface methodology; optimization; tensile strength.

## 1.0 INTRODUCTION

Contemporary materials should possess high mechanical, physical and chemical properties to ensure long and reliable use. The above mentioned requirements and expectations regarding the contemporary materials are met by the non-ferrous metals and alloys such as magnesium alloys. Magnesium alloys and their derivatives, are materials from the lightweight and ultra lightweight family, characterize of low density (1.5–1.8 g/cm<sup>3</sup>) and high strength in relation to their weight. Magnesium and its alloys have a wide prospect for application in the fields of automobiles, electronics and aerospace industry, not only for their light weight but also for their excellent electromagnetic ability. Lightweight magnesium alloys have gradually shifted from military to civil applications during recent years. Especially the AZ series alloys, which contain Al and Zn as the major alloying elements are widely used [1-3]. Gas Tungsten Arc Welding (GTAW) is a widely used material joining process, especially for nonferrous lightweight

metals such as magnesium, aluminium and titanium. The quality of GTA welds ranks higher than that of other arc-welding processes, due to the reliability, clearance and strength of the weld [4]. For magnesium alloys, alternating current (AC) offers a major advantage of cathodic cleaning of the magnesia covering the surfaces over direct current (DC) to initiate a weld pool. However, compared to DC where the electrode is anode and work piece is cathode, AC lowers the heat input to the base metal and produces shallower welds, especially when argon is selected over helium. In pulsed current gas tungsten arc welding (PCGTAW), the welding current is supplied in pulses rather than at a constant magnitude. This is because the conventional tungsten inert gas welding, when used for thin sheets requires very low current, makes the arc wanders from point to point on the surface of the weld pool and or the tip of the electrode. Stability of the arc can be achieved in such cases if the current is supplied in pulses [5].

Various optimization methods can be applied to define the desired output variables through the development of mathematical models to specify the relationship between the input parameters and output variables. One of the most widely used methods to solve this problem is the response surface methodology (RSM), in which the experimenter tries to approximate the unknown mechanism with an appropriate empirical model. A few investigations on the effect of PCGTA welding process parameters and optimization of mechanical and metallurgical properties of aluminium alloy have been reported [8,9]. Very countable number of studies on optimization of PCGTAW arc welding process parameters to attain maximum tensile strength in AZ31B magnesium alloy was available. Hence, in this investigation an attempt was made to develop an empirical relationship to predict tensile strength of PCGTA welded AZ31B magnesium alloy joints using statistical tools such as design of experiments, analysis of variance and regression analysis.

**2.0 DEVELOPING AN EMPIRICAL RELATIONSHIP**

In order to achieve the desired aim, the present investigation was planned in the following sequence:

- (i) Identifying the important PCGTAW parameters that influence tensile strength of the joints
- (ii) Finding the upper and lower limits of the identified parameters.
- (iii) Developing the experimental design matrix.

- (iv) Conducting the experiments as per the design matrix.
- (v) Developing an empirical relationship using response surface methodology.
- (vi) Checking adequacy of the developed relationship.

**2.1 Identifying the important parameters**

From the literature [9, 10] and the preliminary work undertaken, the factors which have significant influence on fusion zone grain refinement and tensile strength of PCGTA welded joints were identified. They are the current ratio, pulse frequency, pulse on time and welding speed.

**2.2 Finding the working limits of the parameters**

A large number of trial experiments were carried out using 3 mm thick rolled sheets of AZ31B magnesium alloy to find out the feasible working limits of PCGTAW parameters. The chemical composition and mechanical properties of the AZ31B magnesium alloy sheets used in this investigation are presented in **Table 1a** and **Table 1b** respectively. Different combinations of PCGTA welding parameters were used to carry out the trial experiments. The weld bead and penetration appearance were inspected to identify the working limits of the welding parameters, leading to the following observations:

1. If current ratio was less than 1.8, then there was incomplete penetration and lack of fusion. For current ratio greater than 2.6, weld dropout occurred.
2. If the pulse frequency was less than 2 Hz, then the bead appearance and bead contours were similar to those of constant current welding. However, if the pulse

**Table 1 (a) : Chemical composition ( wt %) of AZ31B magnesium alloy**

Al	Zn	Mn	Ni	Cr	Cu	Mg
2.60	0.67	0.27	0.012	0.008	0.017	Bal

**Table 1 (b) : Mechanical Properties of AZ31B Magnesium Alloy**

0.2% offset Yield Strength (MPa)	Ultimate tensile strength (MPa)	Elongation in 50 mm gauge length (%)	Reduction in cross section area (%)	Notch tensile strength (MPa)	Notch strength ratio (NSR)	Hardness at 0.05 kg load (Hv)
160	273	14.7	14.3	253	0.92	69

frequency was greater than 6 Hz, arc glare and arc spatter were experienced.

3. If the pulse on time was lower than 30%, weld bead formation was not smooth due to incomplete melting of the base metal. On the contrary, if the pulse on time was greater than 70%, over melting of the base metal and overheating of the tungsten electrode were noticed.
4. If the welding speed was less than 105 mm/min, lack of fusion and depth of penetration were occurred. On contrary, if the welding speed was more than 145 mm/min, weld bead contour and surface breaking defects were encountered.

**2.3. Developing the experimental design matrix**

Feasible limits of the parameters were chosen in such a way that the PCGTAW joints should be free from any visible external defects. The important factors that are influencing the tensile properties of PCGTAW joints and their working range for AZ31B magnesium alloy are presented in **Table 2**. Due to wide range of factors, it was decided to use four factors, five levels, central composite design matrix. **Table 3** shows the 30 sets of coded conditions used to form the design matrix. First 16 experimental conditions are derived from full factorial experimental design matrix ( $2^4 = 16$ ). All the variables at the intermediate (0) level constitute the center points while the combinations of each process variable at either their lowest (-2) or highest (+2) with the other three variables of the intermediate levels constitute the star points. Thus the 30 experimental conditions allowed the estimation of the linear, quadratic and two-way interactive effects of the variables on the tensile strength of PCGTAW joints. The method of designing such matrix is dealt elsewhere [12]. For the convenience of recording and processing experimental data, upper and lower levels of the factors have been coded as +2 and -2 respectively.

**2.4 Conducting the Experiments**

Rolled sheets of AZ31B magnesium alloy of 3 mm thickness were cut into required size of 300 mm × 150 mm × 3 mm by machining. Square butt joint configuration was prepared to fabricate PCGTAW joints. The joint configuration is shown in **Fig. 1**. The initial joint configuration was obtained by securing the plates in position using mechanical clamps. The direction of welding was normal to the rolling direction. Single pass welding procedure was used to fabricate the joints. Argon (purity 99.99%) was used as shielding gas.

The fabricated joints were sliced and then machined to a required size, as shown in **Fig. 2**, according to ASTM E8M-04 standard for sheet type material. The smooth (unnotched) sub size tensile specimens were prepared to evaluate the tensile strength. Photographs of fabricated joints and tensile specimens samples are shown in **Fig. 3**. Tensile test was carried out in an electro-mechanical controlled universal testing machine (FIE-Bluestar, UNITEK-94100) and the average values of three results are presented in **Table 4**.

**2.5 Developing the empirical relationship**

Response surface methodology (RSM) is a collection of mathematical and statistical techniques that is useful for modelling and analyzing problems, in which a response of interest is influenced by several variables and the objective is to optimize this response. The response function of the joint, tensile strength ( $\sigma$ ), is a function of Current Ratio (I), pulse frequency (F), pulse on time (T) and Welding Speed (S), and it can be expressed as:

$$\sigma = f(I, F, T, S) \tag{1}$$

The second order polynomial (regression) equation used to represent the response surface 'Y' is given as:

$$Y = b_0 + \sum b_i x_i + \sum b_{ij} x_i x_j + \sum b_{ijk} x_i x_j x_k + e \tag{2}$$

**Table 2 : Important PCGTAW parameters and their feasible working range**

Parameter	Notation	-2	-1	0	1	2
Current Ratio	I	1.8	2.0	2.2	2.4	2.6
Frequency (Hz)	F	2	3	4	5	6
Pulse on Time (%)	T	30	40	50	60	70
Welding Speed (mm/min)	S	105	115	125	135	145

**Table 3 : Design matrix and experimental results**

Expt. No.	Coded Value				Actual Value				Tensile strength of the joint (MPa)
	R	F	T	S	I	F/Hz	T/%	S/mm/min	
1	-1	-1	-1	-1	1.8	2	30	105	129
2	1	-1	-1	-1	2.4	2	30	105	137
3	-1	1	-1	-1	1.8	5	60	105	148
4	1	1	-1	-1	2.4	5	30	105	169
5	-1	-1	1	-1	1.8	2	30	105	163
6	1	-1	1	-1	2.4	2	30	105	181
7	-1	1	1	-1	1.8	5	60	105	144
8	1	1	1	-1	2.4	5	60	105	173
9	-1	-1	-1	1	1.8	2	30	125	156
10	1	-1	-1	1	2.4	2	30	125	158
11	-1	1	-1	1	1.8	5	30	125	177
12	1	1	-1	1	2.4	5	30	125	190
13	-1	-1	1	1	1.8	2	60	125	170
14	1	-1	1	1	2.4	2	60	125	178
15	-1	1	1	1	1.8	5	60	125	155
16	1	1	1	1	2.4	5	60	125	170
17	-2	0	0	0	2.0	5	50	135	135
18	2	0	0	0	2.6	5	50	135	155
19	0	-2	0	0	2.2	6	50	135	169
20	0	2	0	0	2.2	6	50	135	180
21	0	0	-2	0	2.2	5	40	135	157
22	0	0	2	0	2.2	6	70	135	170
23	0	0	0	-2	2.2	5	30	115	153
24	0	0	0	2	2.2	5	50	145	184
25	0	0	0	0	2.2	5	50	135	214
26	0	0	0	0	2.2	5	50	135	214
27	0	0	0	0	2.2	5	50	135	214
28	0	0	0	0	2.2	5	50	135	210
29	0	0	0	0	2.2	5	50	135	210
30	0	0	0	0	2.2	5	50	135	214

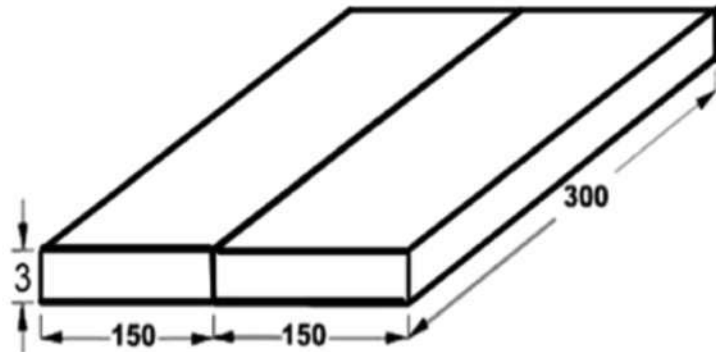
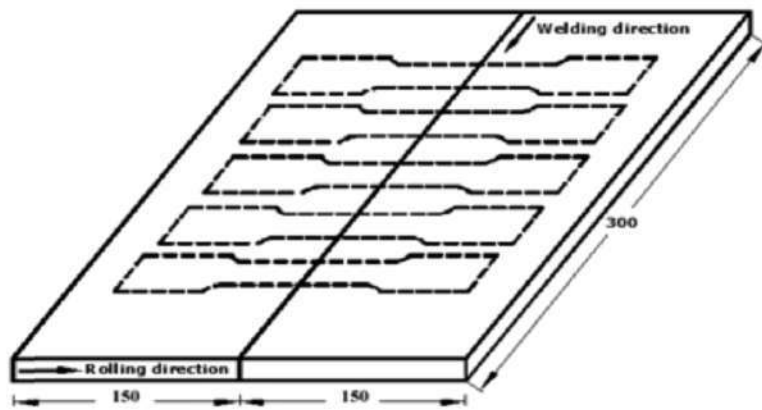
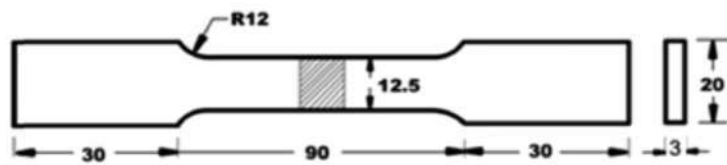


Fig. 1 : Joint configuration

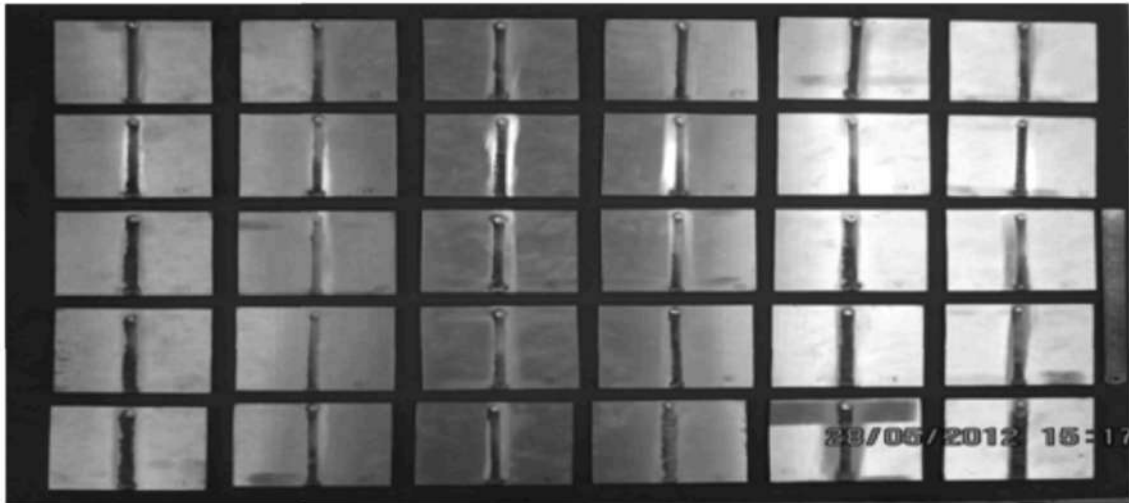


(a) scheme of extraction

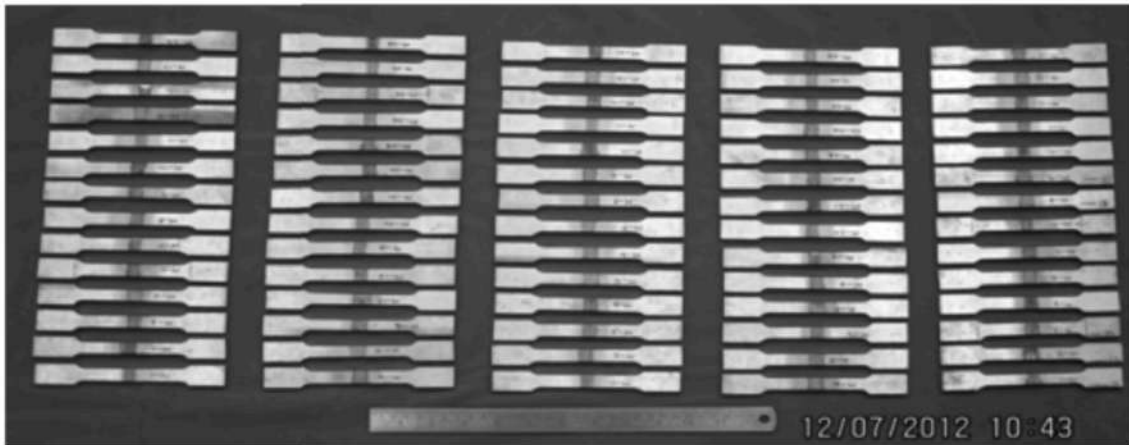


(b) Dimension tensile specimen

Fig. 2 : Dimensions of joint and tensile specimen



( a ) welded joints



( b ) Tensile specimens (before tensile test)



( c ) Tensile specimens (after tensile test)

**Fig. 3 : Photographs of fabricated joints and tensile specimens:**

and for four factors, the selected polynomial could be expressed as:

$$\sigma = b_0 + b_1(I) + b_2(F) + b_3(T) + b_4(S) + b_{11}(I^2) + b_{22}(F^2) + b_{33}(T^2) + b_{44}(S^2) + b_{12}(IF) + b_{13}(IT) + b_{14}(IS) + b_{23}(FT) + b_{24}(FS) + b_{34}(TS) \quad (3)$$

Where  $b_0$  is the average of responses;  $b_i$  and  $b_{ij}$  are the coefficients that depend on the respective main and interaction effects of the parameters. In order to estimate the regression coefficients, a number of experimental design techniques are available. In this work, central composite design which accurately fits the second order response surface was used. All the coefficients were obtained by applying central composite design using the Design Expert statistical software package. After determining significant coefficients, the final relationship was developed using only these coefficients. The final empirical relationship developed by the above procedure to predict tensile strength of PCGTAW AZ31B magnesium alloy is given below:

$$TS = [211.17 + 6.42(I) + 3.12(F) + 4(T) + 7.17(S) + 2.6(I * F) + 1.6(F * T) - 2.4(I)S - 9.6(F * T) + 0.45(F * S) - 5.37(T * S) - 16.62(I^2) - 9.25(F^2) - 12(T^2) - 10.75(S^2)] \text{ MPa} \quad \dots(4)$$

Where,

- Ts = Tensile strength in MPa
- I = Current ratio
- T = Pulse on time (%)
- F = Pulse frequency, Hz
- S = Welding speed, mm/min

**2.6 Checking adequacy of developed relationship**

The adequacy of the developed relationship was tested using the analysis of variance technique (ANOVA). In this technique, if the calculated F value of the developed model is less than the standard F ratio (from F-table) value at a desired level of confidence (95%), the model is adequate within the confidence limit. The ANOVA test results are presented in **Table 5**. It is understood that the developed relationship is adequate at 95% confidence level. The model F-value of 206.7 implies that the relationship is significant. There is only a 0.01% chance that this large "model F-value" could occur due to noise. Values of "prob>F" less than 0.0500 indicate the relationship terms are significant. In this case, I, F, T, S, RF, RT, RS, FT, FS, TS,  $R^2$ ,  $F^2$ ,  $T^2$  and  $S^2$  are significant model terms. Values greater than 0.0001 indicate the relationship terms are not significant. The "lack of fit F-value" of 2.2 implies that the

**Table 4 : ANOVA Test Results**

Source	Sum of Square	Df.	Mean Square	F Value	P-value Prob > F
Model	17357.45	14	1239.818	307.8168	<0.0001
I	988.1667	1	988.1667	245.3379	<0.0001
F	240.6667	1	240.6667	59.75172	< 0.0001
T	384	1	384	95.33793	< 0.0001
S	1232.667	1	1232.667	306.0414	< 0.0001
IF	110.25	1	110.25	27.37241	0.0001
IT	42.25	1	42.25	10.48966	0.0055
IS	90.25	1	90.25	22.4069	0.0003
FT	1482.25	1	1482.25	368.0069	< 0.0001
FS	2.25	1	2.25	0.558621	0.4664
FT	462.25	1	462.25	114.7655	< 0.0001
$I^2$	7581	1	7581	1882.179	< 0.0001
$S^2$	2346.857	1	2346.857	582.668	< 0.0001
$F^2$	3949.714	1	3949.714	980.6187	< 0.0001
$T^2$	3169.714	1	3169.714	786.9635	< 0.0001

Residual	60.41667	15	4.027778		
Lack of Fit	49.58333	10	4.958333	2.288462	0.1868
Pure Error	10.83333	5	2.166667		
Cor Total	17417.87	29			

Std. Dev.	2.006932	R-Squared	0.996531
Mean	172.2667	Adj R-Squared	0.993294
C.V. %	1.165015	Pred R-Squared	0.982707
PRESS	301.2	Adeq Precision	57.87055

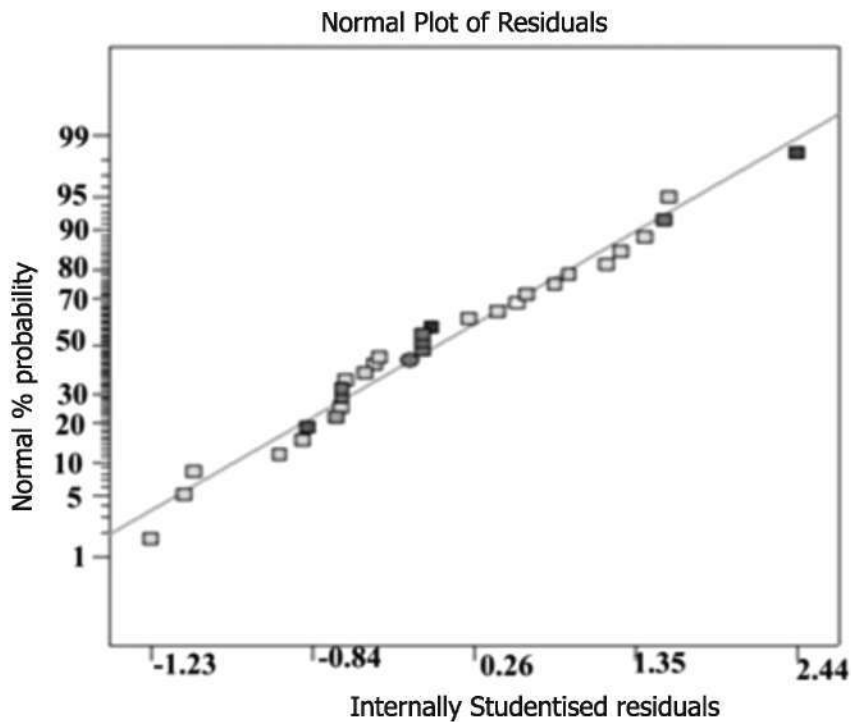


**Fig. 4 : Normal probability plot of residuals**

lack of fit is not significant compared to the pure error. There is a 18.68% chance that a large "lack of fit F-value" could occur due to noise. Coefficient of determination " $R^2$ " is used to find how close the predicted and experimental values lie. The value of " $R^2$ " for the above-developed relationship is also presented in **Table 5**, which indicates high correlation existing between the experimental values and predicted values. The "Pred. R-squared" of 0.973 is in reasonable agreement with the 'adj R-

squared' of 0.982. "Adeq precision" measures the signal to noise ratio. The normal probability plots of the residuals for tensile strength are shown in **Fig.4** which reveals the residuals are falling on the straight line, indicating the errors are distributed normally [13]. All the above consideration indicates an excellent adequacy of the developed empirical relationship. Each observed value is compared with the predicted value calculated from the relationship in **Fig.5**.



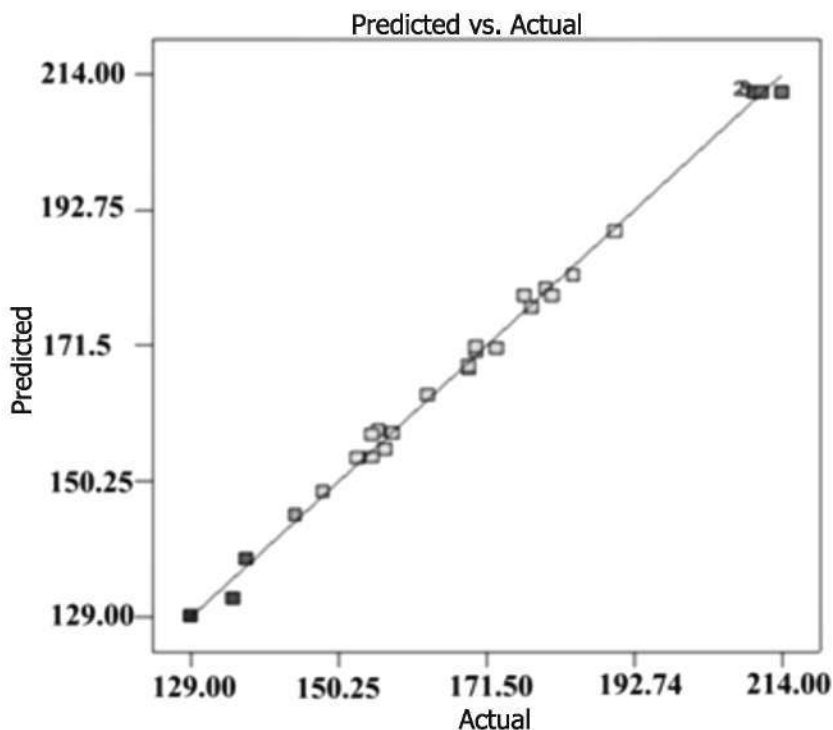


Fig. 5 : Correlation graph

Table 5 : Validation results for developed empirical relationships

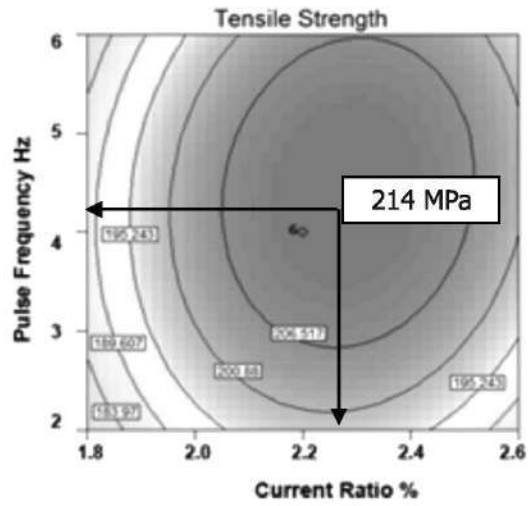
Expt. No.	Current ratio (I)	Pulse frequency (F)	Pulse on time (%)	Welding speed (mm/min)	By experiment	By model	Variation (%)
1	1.9	2.5	35	110	170	173.6	2.11
2	2.1	3.5	45	120	186	183.64	-1.34
3	2.3	4.5	55	130	191	194.21	-3.08

### 3.0 OPTIMIZATION OF PCGTAW PARAMETERS

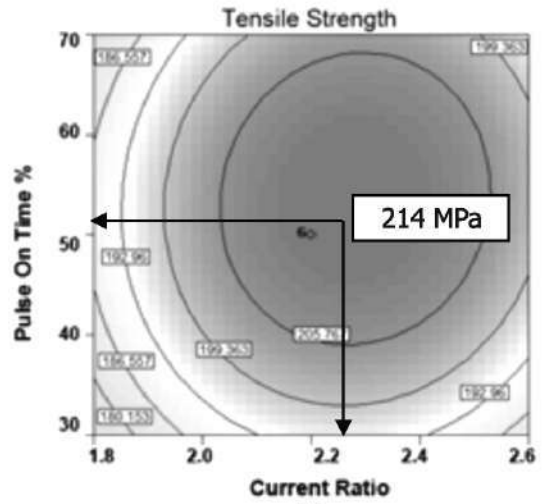
The response surface methodology (RSM) was used as an optimization tool to search the optimum values of the process variables. The empirical relationship developed in the previous section was framed using the coded values. The optimization was done on coded values and then converted to actual values. Design Expert version statistical software package was used to optimize the process variables. The optimum values obtained are listed in **Table 6**. Under the optimum conditions, a maximum tensile strength of 214 MPa was obtained.

Response surfaces were developed for the empirical relationship, taking two parameters in the 'X' and 'Y' axes and response in 'Z' axis. The response surfaces clearly indicate the

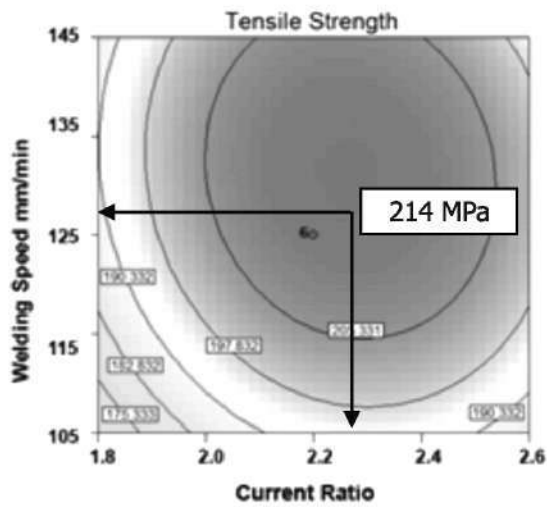
optimal response point. The optimum tensile strength of PCGTA welded AZ31B magnesium alloy was exhibited by the apex of the response surface, as shown in **Fig. 6**. Contour plots show distinctive circular mound shape which is indicative of possible independence of factors with response to display the region of optimal factor settings. By generating contour plots using software for response surface analysis, the optimum is located with reasonable accuracy by characterizing the shape of the surface. If a contour patterning of circular shaped contour occurs, it tends to suggest the independence of factor effects while elliptical contours may indicate factor interactions [14]. The optimum response for PCGTA welded AZ31B magnesium alloy is shown in **Fig. 7**.



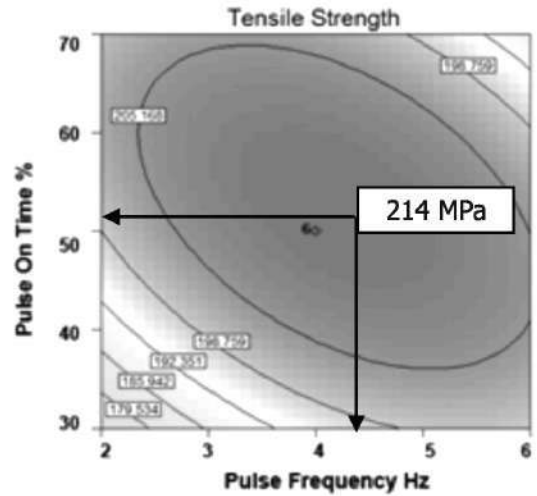
(a)



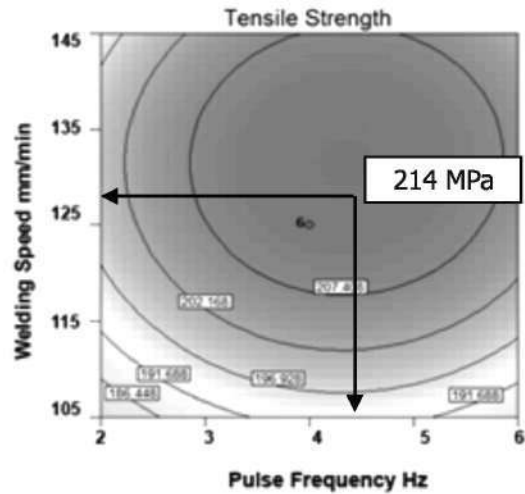
(b)



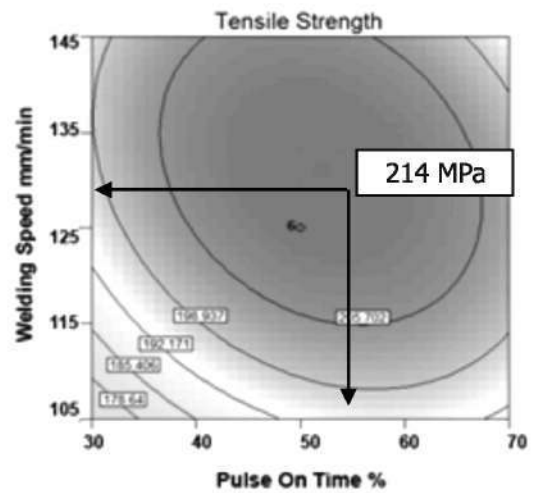
(c)



(d)



(e)



(f)

Fig. 6 : Contour plots for PCGTA welded AZ31B magnesium alloy

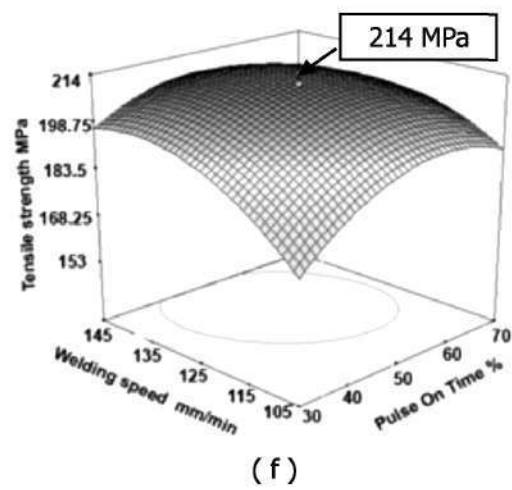
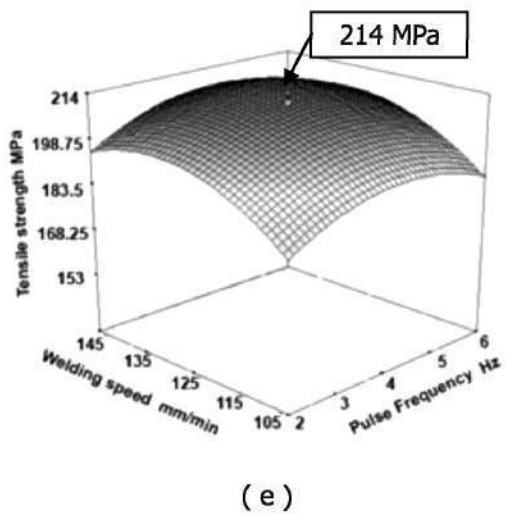
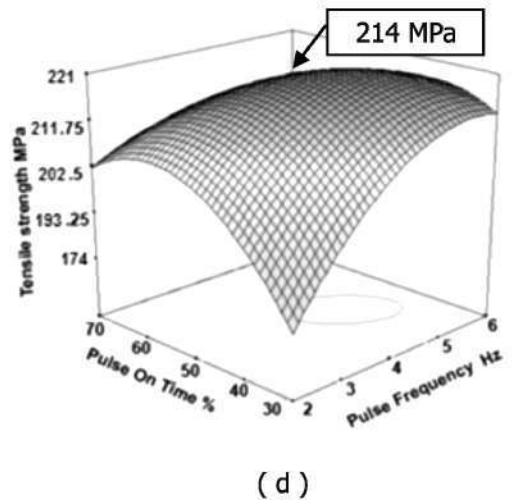
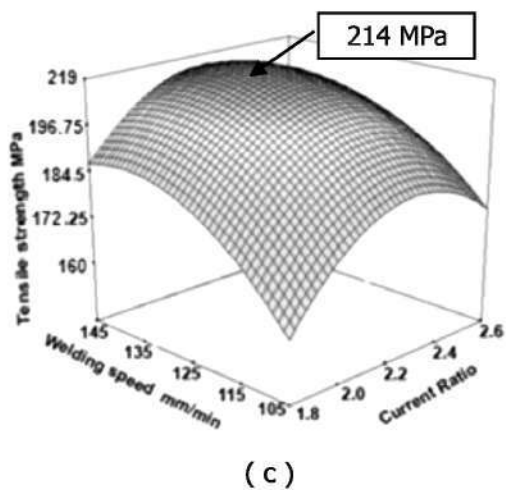
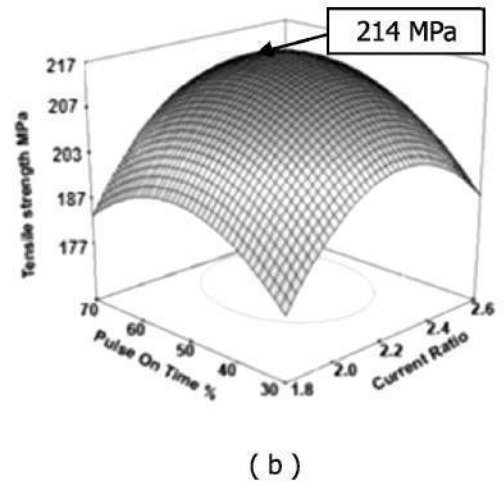
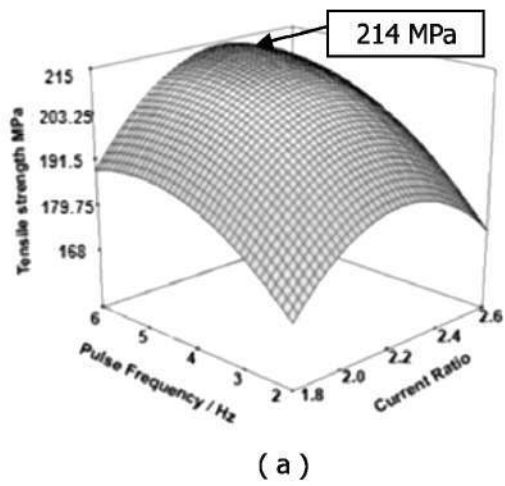


Fig. 7 : Response graphs for PCGTA welded AZ31B magnesium alloy

#### 4.0 ANALYSIS OF RESPONSE GRAPHS AND CONTOUR PLOTS

By generating response graphs and contour plots using Design Expert software for response surface analysis, it is easy to locate the optimum conditions with reasonable precision. **Fig. 6 (a)** shows the three dimensional response surface plot for the response tensile strength obtained from the regression model, assuming a current ratio of 2.2 and pulse frequency of 5 Hz. The optimum tensile strength is exhibited by the apex of the response surface. From the response graph, it is identified that at the current ratio of 2.2, the tensile strength of PCGTAW joints is higher. The formation of fine equiaxed grains in fusion zone increases the tensile strength of these joints. When the current ratio is increased from of 2.2, the tensile strength decreases. This is the result of the increased heat input associated with the use of higher current ratio. The formation of coarser grains in the fusion zone is responsible for the lower tensile properties of these joints. This phenomenon can be also explained by the change of cooling rate. It is known that an increase in heat input results in slow cooling rate. Moreover, the slower the cooling rate during solidification, the longer the time available for grain coarsening. In contrast, the decrease in current ratio leads to the decrease in heat input which leads to faster cooling rate and subsequently finer grain size in fusion zone [13].

**Fig.6 (b)** it is identified that at the pulse on time of 50%, the tensile strength of PCGTAW joints is higher. The fine grains observed in the fusion zone may be responsible for higher tensile strength of these joints. This is mainly due to the optimum heat input. The pulse on time increases further, which promotes the grain growth on the weld region. This is because as the pulse on time increases, the period from the start of a pulse to the end of the base time also increases. When the pulsing time is increased, the welding heat has more time to conduct into the fusion zone, which promotes grain coarsening [16]. The grains in fusion zone get coarser, with increasing pulse on time, and the tensile strength of these joints decreases.

**Fig. 6 (c)** shows the three dimensional response surface plot for the response tensile strength obtained from the regression model, assuming a welding speed of 135 mm/min and current ratio of 2.2. From the response graph, it is identified that at the welding speed of 135 mm/min the tensile strength of PCGTAW joints is higher. When the welding speed is decreased from of 135 mm/min, the tensile strength decreases. This is the result of the increased heat input associated with the use of slower welding speed. The formation of coarser grains in the fusion

zone is responsible for the lower tensile properties of these joints. This phenomenon can be also explained by the change of cooling rate. It is known that an increase in heat input results in slow cooling rate. Moreover, the slower the cooling rate during solidification, the longer the time available for grain coarsening. In contrast, the increase in welding speed leads to the decrease in heat input, which leads to faster cooling rate and subsequently finer grain size in fusion zone [13].

**Fig.6 (d)** shows the three dimensional response surface plots for the response tensile strength obtained from the regression model, assuming a pulse frequency of 5 Hz and a pulse on time of 50 %. Increases further, which promotes the grain growth on the weld region. This is because as the pulse on time increases, the period from the start of a pulse to the end of the base time also increases. When the pulsing time is increased, the welding heat has more time to conduct into the fusion zone, which promotes grain coarsening [16]. At high frequencies, the vibration amplitude and temperature oscillation induced on the weld pool are reduced to a greater extent resulting in reduced effect on the weld pool. Moreover, at high pulse frequency values, the molten pool is agitated violently, resulting in grain refinement in the weld region [15]. Hence, there exists an optimum pulse frequency at which the grain refinement is maximum. In this investigation, the optimum pulse current frequency is found to be 5 Hz.

#### 4.1 Validation of developed empirical relationships

In the development of empirical relationships, it is important to determine whether the developed relationships meet the specifications and the prediction are correct. The prediction capability of developed empirical relationships was validated by conducting three more experiments using welding parameter combinations that are not prescribed by the design matrix (**Table 4**). The experimental and predicted results are presented in **Table 6**. Predicted tensile strength obtained using developed in relationship have good agreement with the experimental values and the variation is found to be within  $\pm 5\%$ . From the above results, it is concluded that the developed relationship can be effectively used to predict tensile strength of GTA welded AZ 31B welded joints at 95% confidence level.

#### 4.2 Validation of optimization procedures

The confirmatory experiments were conducted with the welding parameters as suggested by the numerical modelling (suggested solutions) and keeping the current ratio, pulse frequency, pulse on time and welding speed at 2.24, 4.18 Hz, 50.4 % and 128.1mm/min respectively. A very small difference

was found between the predicted values and experimental values (**Table 7**). Further, additional two set of experiments were conducted above and below the optimized welding conditions and observed results were presented in the **Table 7**. Optimized parameters are shown in **Table 8**. From these

results, it is observed that deviating welding parameters from the optimized conditions leads to decreased tensile strength due to insufficient higher heat input reflecting in the grains evolution at the microstructure level.

**Table 6 : Validation results for optimisation procedure**

Expt. No.	Current ratio (I)	Pulse frequency (F)	Pulse on time (%)	Welding speed (mm/min)	By experiment	By model	Variation (%)
1	1.9	3.5	41	117	202	210.64	4.8
2	2.24	4.18	50.5	128	208	212.6	2.0%

**Table 7 : Optimized parameters**

Parameter	Current ratio	Pulse frequency (Hz)	Pulse on time (%)	Welding speed (mm / min)
	2.2	5	50	135

## 5.0 CONCLUSIONS

- 1) An empirical relationship was developed to predict tensile strength of pulsed current gas tungsten arc welded AZ31B magnesium alloy joints using response surface methodology. Incorporating welds parameters the developed relationship can be effectively used to predict the tensile strength of PCGTAW joints of AZ31B magnesium alloy at 95% confidence level.
- 2) A maximum tensile strength of 214 Mpa (78% of base metal strength) was obtained under the welding condition of current ratio of 2.2, pulse frequency of 5 Hz, pulse on time of 50% and welding speed of 135 mm/min which is the optimum PCGTAW welding condition for AZ31B magnesium alloy.
- 3) From the analysis of variance (ANOVA) test results and from the F ratio it is found that the welding speed has the greatest influence on tensile strength, followed by current ratio, pulse on time and pulse frequency.

## ACKNOWLEDGMENTS

The authors wish to place their sincere thanks to University Grant Commission (UGC), New Delhi for financial support rendered through Major Research Project No: 39-864/2010.

## REFERENCES

1. L. A. Dobrzański, T. Tański, L. Cizek, Z. (2007); Journal of Materials Processing Technology 192–193:567–574
2. Zhang Zhi-min, XU Hong-yan, Wang. (2008); Corrosion and mechanical properties of hot-extruded AZ31 magnesium alloys., Transactions of Non Ferrous Metals Society of China 18 :s140-s144
3. L. D. Scintilla, L. Tricarico, M. Brandizzi, A. A. Satriano, (2010); Nd:YAG laser weldability and mechanical properties of AZ31 magnesium alloy butt joints, Journal of Materials Processing Technology 2206–2214
4. G. Padmanaban, V. Balasubramanian (2007); Optimization of pulsed current gas tungsten arc welding process parameters to attain maximum tensile strength in AZ31B magnesium alloy. Transactions of Non Ferrous Metals Society of China 21:467-476
5. A. Razal Rose, K. Manisekar, V. Balasubramanian, S. Rajakumar (2012); Prediction and optimization of pulsed current tungsten inert gas welding parameters to attain maximum tensile strength in AZ61A magnesium alloy., Materials and Design 37:334–348

6. T. S. Balasubramanian, M. Balakrishnan, V. Balasubramanian, M. A. Muthu Manickam. (2011); Influence of welding processes on microstructure, tensile and impact properties of Ti-6Al-4V alloy joints. Transactions of Non Ferrous Metals Society of China 21: 1253-1262
7. S. Kou, Y. Le (1986); Nucleation mechanism and grain refining of weld metal. Welding Journal 65(4):65-70
8. T. Senthil Kumar, V. Balasubramanian, M. Y. Sanavullah (2007); Influences of pulsed current tungsten inert gas welding parameters on the tensile properties of AA6061 aluminum alloy. Materials and Design 28:2080-92.
9. I. M. Liu, Z. D. Zhang, G. Song, L. Wang (2006); Mechanism and microstructure of oxide fluxes for gas tungsten arc welding of magnesium alloy. Metallurgical and Materials Transactions A, , 38: 649-658.
10. J. Shen, G. Q. You, S. Y. Long, F. S. Pan (2008); Abnormal macropore formation during double-sided gas tungsten arc welding of magnesium AZ91D alloy. Materials Characterization, 59 (8): 1059-1065.
11. G. E. P. Box, W. H. Hunter, J. S. Hunter; Statistics for experiments [M]. (1978); New York: John Wiley Publications,
12. S. Kumar, P. Kumar, H. S. Shan (2007); Effect of evaporative casting process parameters on the surface roughness of Al-7%Si alloy castings. Materials Processing and Technology,182: 615-623.
13. D. C. Montgomery; Design and analysis of experiments [M]. (2001); New York: John Wiley & Sons.
14. S. Kou, Y. Le (1986) Nucleation mechanism and grain refining of weldmetal, Welding Journal 65-70.
15. G. Padmanaban and V. Balasubramanian. (2011); Influences of Pulsed Current Parameters on Mechanical and Metallurgical Properties of Gas Tungsten Arc Welded AZ31B Magnesium Alloys, Metals and Materials International., 17 (5) pp. 831-839.
16. A. Munitz, C. Cotler, A. Stern, G. Kohn . (2001); Mechanical properties and microstructure of gas tungsten arc welded magnesium AZ91D plates, Materials Science and Engineering A302:68-73.